BIOCHEMICAL PHARMACOLOGY 76 (2008) 1563–1576

available at www.sciencedirect.com

ScienceDirect

journal homepage: www.elsevier.com/locate/biochempharm

# Regulation of antiapoptotic MCL-1 function by gossypol: Mechanistic insights from in vitro reconstituted systems

*Aitor Etxebarria* [a], *Olatz Landeta* [a], *Bruno Antonsson* [b], *Gorka Basañez* [a,*]

[a] *Unidad de Biofísica (CSIC-UPV/EHU), Universidad del Pais Vasco/Euskal Herriko Unibertsitatea (UPV/EHU), P.O. Box 644, 48080 Bilbao, Spain*

[b] *Merck Serono International, S. A., 9 chemin des Mines, 1202 Geneva, Switzerland*

ARTICLE INFO

*Article history:*
Received 8 June 2008
Accepted 5 August 2008

*Keywords:*
BCl-2
MCL-1
Gossypol
Apoptosis
Cancer

ABSTRACT

Small-molecule drugs that induce apoptosis in tumor cells by activation of the BCL-2-regulated mitochondrial outer membrane permeabilization (MOMP) pathway hold promise for rational anticancer therapies. Accumulating evidence indicates that the natural product gossypol and its derivatives can kill tumor cells by targeting antiapoptotic BCL-2 family members in such a manner as to trigger MOMP. However, due to the inherent complexity of the cellular apoptotic network, the precise mechanisms by which interactions between gossypol and individual BCL-2 family members lead to MOMP remain poorly understood. Here, we used simplified systems bearing physiological relevance to examine the impact of gossypol on the function of MCL-1, a key determinant for survival of various human malignancies that has become a highly attractive target for anticancer drug design. First, using a reconstituted liposomal system that recapitulates basic aspects of the BCL-2-regulated MOMP pathway, we demonstrate that MCL-1 inhibits BAX permeabilizing function via a ''dual-interaction'' mechanism, while submicromolar concentrations of gossypol reverse MCL-1-mediated inhibition of functional BAX activation. Solution-based studies showed that gossypol competes with BAX/BID BH3 ligands for binding to MCL-1 hydrophobic groove, thereby providing with a mechanistic explanation for how gossypol restores BAX permeabilizing function in the presence of MCL-1. By contrast, no evidence was found indicating that gossypol transforms MCL-1 into a BAX-like pore-forming molecule. Altogether, our findings validate MCL-1 as a direct target of gossypol, and highlight that making this antiapoptotic protein unable to inhibit BAX-driven MOMP may represent one important mechanism by which gossypol exerts its cytotoxic effect in selected cancer cells.



## 1. Introduction

The control of apoptosis is largely governed by the BCL-2 protein family, whose principle function during cell death is to modulate the MOMP process allowing for the release of apoptogenic factors, such as cytochrome c and AIF, into the cytosol [1]. MOMP is regarded as the crucial point that irreversibly commits a cell to death by apoptosis [2]. BCL-2 family members can be classified according to their impact on this key event determining cell viability, and to the presence of up to four evolutionarily conserved homology regions (BH domains) [1,2]. BAX and its close homologue BAK constitute a first sub-group of proapoptotic family members (BAX-type proteins), which are characterized by being the effectors of

* *Corresponding author at*: Unidad de Biofísica (CSIC-UPV/EHU), Barrio Sarriena, s/n, Leioa 48940, Spain. Tel.: +34 946013355; fax: +34 946013360.
E-mail address: gbzbaasg@lg.ehu.es (G. Basañez).

0006-2952/$ – see front matter © 2008 Elsevier Inc. All rights reserved.
doi:10.1016/j.bcp.2008.08.003

MOMP and by containing BH1–BH3 domains. A second, more diverse sub-group of proapoptotic molecules comprises more than eight members, including tBID and BIM, which assist BAX-type proteins to elicit MOMP and possess only the third BH domain (BH3-only proteins). Finally, the antiapoptotic sub-group of BCL-2 family proteins includes BCL-2, BCL-$X_L$, BCL-W, BFL-1, and MCL-1 (BCL-2 type proteins), which act by inhibiting MOMP and display sequence homology in all BH1–BH4 domains. Of note, overexpression of BCL-2 type proteins commonly occurs in human malignancies and is usually associated with disease maintenance and progression, resistance to chemotherapy, and poor clinical outcome [1,3]. These antiapoptotic proteins thus represent promising candidates for therapeutic intervention.

It has long been recognized that heterodimerization of BCL-2 type proteins with proapoptotic family members is pivotal to preservation of cell viability. Solution-based structural and binding studies revealed that BH1, BH2, and BH3 domains in antiapoptotic proteins form a surface-exposed hydrophobic groove, which can accommodate BH3 domains from proapoptotic partners [4]. One potential downside of these investigations is that the behavior of soluble BCL-2 proteins may not fully reveal their mechanisms of action at the outer mitochondrial membrane (MOM) locus. In line with this, the precise mechanisms by which protein–protein interactions among opposing factions of the BCL-2 family lead to inhibition of MOMP remain controversial [1–6]. Notwithstanding these caveats, over the past years a number of natural and synthetic small molecules have been identified with potential to compete with proapoptotic BH3 ligands for binding to BCL-2 type proteins, creating interest in these compounds as putative new anticancer drugs [3,7]. A prominent example is the compound ABT-737 designed by Abbott laboratories, which has been shown to associate with high affinity to the hydrophobic groove of BCL-2, BCL-$X_L$, and BCL-W in solution, and potently kills selected cancer cells overexpressing these antiapoptotic proteins as a single agent or in combination therapies [8–16]. Importantly, resistance to ABT-737 treatment appears to correlate with MCL-1 expression levels, consistent with biochemical data demonstrating that ABT-737 does not bind to MCL-1 [17–22]. Additional studies indicate that MCL-1 is an important survival factor for many human malignancies, its expression contributing to resistance to a variety of anticancer therapies [23–30]. Taken together, these observations warrant a deeper understanding of the mechanism by which MCL-1 inhibits MOMP, as well as the identification and characterization of small-molecule compounds that neutralize MCL-1's antiapoptotic function.

Gossypol is a natural polyphenol derived from the cotton plant that is currently being clinically evaluated as an anticancer agent [3]. Evidence is accumulating that gossypol and derivative compounds kill multiple tumor cell lines, at least in part, by activating the BCL-2-regulated apoptotic pathway [31–39]. However, important aspects of the mechanism by which gossypol affects BCL-2 protein function remain unclear. Specifically, most studies performed to date have focused in examining the molecular underpinnings by which putative binding interactions between gossypol and BCL-2 or BCL-$X_L$ influence global apoptosis susceptibility. Additionally, evidence exists indicating that gossypol affects the viability of cells lacking BAX-type proteins [17], and that this compound can convert BCL-2/BCL-$X_L$ into BAX-like proapoptotic molecules capable of directly eliciting MOMP [33]. Taken together, these studies leave open the important question of how the specific interaction of gossypol with MCL-1 might impact on MOM permeability.

Due to the complexity of the apoptotic network, simplified cell-free systems have proved to be valuable tools that complement in vivo cell biology approaches for revealing the mode of action of individual BCL-2 family members [6]. Here, we used an array of in vitro reconstituted systems to advance in our knowledge of the molecular basis underlying MCL-1-mediated inhibition of MOMP, and to analyze the potential impact of gossypol on MCL-1's function from a mechanistic viewpoint. Our results are consistent with a ''dual-interaction'' mode of MCL-1 action, whereby complexation of MCL-1 with either BAX or tBID leads to inhibition of BAX permeabilizing function. We also found that gossypol competes with both BAX BH3 and tBID BH3 ligands for binding to the hydrophobic groove of MCL-1, thereby providing with a mechanistic explanation for how this compound reverses MCL-1's inhibitory effect on functional BAX activation. In addition, several lines of evidence are presented suggesting that gossypol does not act by changing MCL-1 conformation in such a manner as to unleash a BAX-like pore-forming activity. Altogether, our observations add significantly to a growing body of evidence indicating that gossypol elicits its antitumor activity, at least in part, through functional blockade of BCL-2 type proteins with consequent activation of BAX-driven MOMP.

## 2. Materials and methods

### 2.1. Materials

KCl, HEPES, EDTA, dodecyl octaethylene glycol monoether ($C_{12}E_8$), fluorescein isothiocyanate-labeled dextrans of 70 kDa (FD70), guanidinium hydrocloride (GuHCl), gossypol (racemic mixture of two enantiomers (−)gossypol and (+) gossypol, purity ≥95% as determined by HPLC), epigallocathecin, and chelerytrine, were obtained from Sigma–Aldrich (St. Louis, MO). Egg phosphatidylcholine (PC), 1, 2-distearoyl-9,10-dibromo-SN-glycero-3-phosphocholine (Br-PC), egg phosphatidylethanolamine (PE), liver phosphatidylinositol (PI), and heart cardiolipin (CL), were purchased from Avanti Polar Lipids, Inc (Alabaster, AL). 8-aminonaphthalene-1,3,6-trisulfonate (ANTS), and 45 mM *p*-xylene bis(pyridinium bromide) (DPX) were purchased from Molecular Probes (Eugene, OR).

### 2.2. Recombinant proteins and synthetic peptides

All proteins were purified from soluble fractions of bacterial extracts obtained in the absence of detergents, and were >90% pure as evaluated by Coomassie-stained SDS-PAGE. Recombinant purified hexahistidine ($His_6$)-tagged full-length monomeric BAX (BAX), recombinant purified caspase-8-cleaved BID (tBID), recombinant purified $His_6$-tagged human $BIM_L$ lacking the C-terminal 27 aminoacids ($BIM_L$), and recombinant purified MCL-1 lacking the N-terminal 151 aminoacids and

the C-terminal 23 aminoacids (MCL-1) were obtained as described previously [40]. The plasmid for expression of MCL-1 was a generous gift of D. Huang. HPLC-purified peptides were obtained from Abgent (San Diego, CA). Peptide sequences were as follows: BAX BH3, ASTKKLSECLKRIGDELDSNMELQRMIAA; BAX BH3 mt, ASTKKLSECAKRIGAELDSNMELQRMIAA; BID BH3, IIRNIARHLAQVGDSMDRSIPPGLVNGLA; BID BH3 mt, DIIRNIARHAAQVGASMDRSIPPGLVNGLA; fluorescein isothyacianate-conjugated BAX BH3 (F-BAX BH3), F-Ahx-STKKLSECLKRIGDELDSNMELQR; fluorescein isothyacianate-conjugated BID BH3 (F-BID BH3), F-Ahx-IRNIARHLAQVGDSMDRSIPP; and fluorescein isothyacianate-conjugated BIM BH3 (F-BIM BH3), F-Ahx-EIWIAQELRRIGDEFNETYTR. Peptide identity was confirmed by electrospray mass spectroscopy.

### 2.3. Cytochrome c release assays

Mitochondria were isolated from livers of male Harlan Sprague-Dawley rats as described previously [41], and used within 3 h. Isolated mitochondria (500 μg of protein/ml) were incubated with recombinant proteins in 50 μl of 25 mM KCl, 5 mM $KH_2PO_4$, 25 μM EGTA, 5 mM succinate, 5 μM rotenone, and 10 mM HEPES-KOH, pH 7.2, under constant stirring and 30 °C, using an Eppendorf Thermomixer. MCL-1 was first incubated with mitochondria for 5 min, followed by addition of proapoptotic proteins, and further incubation of the sample for 20 min. Reaction mixtures were centrifuged at 14,000 × *g* for 10 min to isolate the pellet and supernatant fractions, and cytochrome *c* contents were determined quantitatively using a colorimetric ELISA assay (R&D Systems, Minneapolis, MN). The percentage of cytochrome *c* released into the supernatant (%cyto *c*) was calculated according to the following equation: %cyto $c = ([\text{cyto } c_{sup} - \text{cyto } c_{backgr}]/[\text{cyto } c_{total} - \text{cyto } c_{bacgr})] \times 100$, where background release represents cytochrome *c* detected in the supernatant of buffer-treated samples and total release represents cytochrome *c* measured in Triton X-100-treated samples. Absorbance measurements were carried on a Biotek Synergy HT fluorescence microplate reader.

### 2.4. Liposome preparation

Liposomes were prepared with a lipid composition resembling that of MOM contact sites [(40 PC/35 PE/10 PI/15 CL (mol/mol)] (MOM-like liposomes). Lipid mixtures at the indicated ratios were co-dissolved in chloroform/methanol (2:1), and organic solvents were removed by evaporation under an argon stream followed by incubation under vacuum for 2 h. For assays of vesicular release, dry lipid films were resuspended either in 100 mM KCl, 10 mM Hepes pH 7.0, 0.1 mM EDTA (KHE buffer) supplemented with 100 mg/ml FD70, or in 12.5 mM ANTS, 45 mM DPX, 20 mM KCl, 10 mM HEPES, 0.1 mM EDTA, pH 7.0. For other assays dry lipid films were resuspended in KHE. Multilamellar vesicles were then subjected to five freeze/thaw cycles. These frozen/thawed liposomes were used in direct protein-binding assays. In all other assays, large unilamellar vesicles (LUV) were used, produced by 10× extrusion through two polycarbonate membranes of 0.2-μm pore size (Nucleopore, San Diego, CA). Untrapped ANTS/DPX and FD70 were removed by gel filtration in Sephadex G-25 and Sephacryl S-500 HR columns, respectively, with KHE running as elution buffer.

### 2.5. Fluorimetric measurements of vesicular contents release

Release of LUV-encapsulated fluorescent markers was monitored in an 8100 Aminco-Bowman luminescence spectrometer (Spectronic Instruments, Rochester, NY) in a thermostatted 1-cm path length cuvette with constant stirring, at 37 °C. For FD70, $\lambda_{ex}$ was 490, and $\lambda_{em}$ was 520 nm (slits, 4 nm); for ANTS/DPX, $\lambda_{ex}$ was 350 nm, and $\lambda_{em}$ was 520 nm (slits, 8 nm). A 515 nm cut-off filter was placed between the sample and the emission monochromator to avoid scattering interferences. MCL-1 was first incubated with or without gossypol for 5 min, followed by addition of liposomes and incubation for another 5 min, prior to treatment with proapoptotic proteins. The extent of marker release was quantified on a percentage basis according to the equation: $(F_t - F_0/F_{100} - F_0) = 100$ where $F_t$ is the measured fluorescence of protein-treated LUV at time t, $F_0$ is the initial fluorescence of the LUV suspension before protein addition, and $F_{100}$ is the fluorescence value after complete disruption of LUV by addition of $C_{12}E_8$ (final concentration, 0.5 mM). Lipid concentration was 50 μM.

### 2.6. Binding of proteins to MOM-like liposomes

To assay the liposome binding capacity of multiple BCL-2 proteins present in the same sample, a low-speed vesicle sedimentation approach was used followed by protein detection by immunoblotting. MCL-1 was first incubated with or without gossypol for 5 min, followed by addition of freeze/thawed vesicles and incubation for another 5 min. Then, proapoptotic proteins were added and the mixture was further incubated for another 30 min. Incubations were done under constant stirring at 37 °C, using an Eppenford Thermomixer. Next, the mixture was centrifuged for 30 min at 18,000 × *g*, 4 °C, and equivalent aliquots were taken from supernatant (corresponding to free protein) and pellet fractions (corresponding to liposome-bound protein). Both fractions were then subjected to reducing SDS-PAGE on 15% Tris–glycine gels, followed by visualization by Western blotting using appropriate primary antibodies, peroxidase-conjugated secondary antibodies, and enhanced-chemiluminescent (ECL) kit substrates (Pierce). Primary antibodies used for BAX, tBID and MCL-1 detection were anti BID MAB860 monoclonal antibody (R&D systems), anti BAX N20 polyclonal antibody (Santa Cruz), and anti MCL-1 AF828 polyclonal antibody (R&D systems), respectively.

The utility of the above-described approach is limited by the semi-quantitative nature of Western blotting as a method for estimation of protein content, and by the fact that this procedure does not allow complete separation of lipid-containing and lipid-free fractions [40]. To assess MCL-1 association with MOM-like liposomes in a more quantitative manner, a different assay was used which also ensures complete sedimentation of lipid vesicles [42]. Briefly, freeze/thawed MOM-like liposomes were prepared in which PC was substituted for Br-PC, and compounds of interest were

incubated overnight with lipid vesicles under constant stirring in low-binding eppendorf tubes, at 37 °C ($V_{final}$ = 1 ml). The mixture was then centrifuged by a three-step low-speed centrifugation (4000, 9000, 18,000 × *g*), for 30 min each. At the end of the centrifugation, the supernatant was removed from the tube and assayed for total protein concentration by the Bradford method. A standard curve for the Bradford assay was generated from known concentrations of MCL-1, and the percentage of protein bound to the vesicles was estimated using the difference between the amount of protein used in the reaction and the amount of protein remaining in the supernatant.

### 2.7. Steady-state fluorescence spectroscopy

Association of gossypol to MCL-1 was monitored by observing the protein emission spectrum from tryptophan fluorescence. Sample components were incubated for 10 min prior to beginning of measurents. The excitation wavelength was 290 nm and the emission spectrum was collected between 300 nm and 450 nm at a scan rate of 1 nm/s. The slit widths for excitation and emission were kept at 4 nm, with the experiment conducted at 37 °C. The contribution of buffer to sample fluorescence was substracted as blank.

To assess the thermodymanic stability of MCL-1 by chemical denaturation studies, sample components were incubated for 1 h in KHE buffer at 37 °C prior to beginning of measurents. Protein fractional denaturation ($F_D$) was determined with increasing GuHCl concentrations:

$$F_D = \frac{(\lambda_x - \lambda_N)}{(\lambda_D - \lambda_N)}$$

where $\lambda_x$, $\lambda_N$, and $\lambda_D$, are, respectively, the maximum fluorescence emission wavelengths of the protein Trp residues, of a partially denatured ($\lambda_x$), totally denatured ($\lambda_D$), or native protein ($\lambda_N$).

The denaturation constant is:

$$K_D = \frac{F_D}{F_N} = \frac{F_D}{1 - F_D}$$

$$\text{Thus, } \Delta G_D^\circ = -RT\ln K_D$$

To calculate $\Delta G^\circ$ ($H_2O$), the Gibbs free energy of protein unfolding in the absence of GuHCl, the $\Delta G_D^\circ$ values obtained for GuHCl concentrations within the transition zone of the denaturation curve were used to fit the equation

$$\Delta G^\circ(H_2O) = \Delta G_D^\circ - m_G[\text{GuHCl}],$$

where $m_G$ is an indicator of the extent to which the denatured state interacts with GuHCl.

### 2.8. Fluorescence polarization (FP) assays

FP-based binding assays were performed in a Perkin Elmer 8100 spectrofluorimeter at 37 °C. In direct-binding FP measurements, MCL-1 (400 nM) was incubated for 30 min with F-BH3 peptides (5 nM). In competition-binding FP measurements, MCL-1 (400 nM) was first incubated for 10 min with various concentrations of gossypol, followed by addition of F-BH3 peptides (5 nM), and further incubation of the mixture for another 30 min. $EC_{50}$ and $IC_{50}$ values were determined by fitting the experimental data using a sigmoidal dose–response nonlinear regression model with Sigma Plot software.

### 2.9. Far-UV circular dichroism (CD) measurements

Far-UV CD spectra were recorded at 37 °C on a Jasco J-810 spectrapolarimeter (Jasco Spectroscopic Co. Ltd., Hachioji City, Japan) equipped with a JASCO PTC-423S temperature control unit, using 1-mm pathlength cell. Data were collected every 0.2 nm at 50 nm/min from 250 nm to 200 nm, with a bandwidth of 2 nm, and results were averaged from 20 scans. Preparations of MCL-1 were used in 5 mM Hepes, pH 7.0. All samples were allowed to equilibrate for 10 min prior to CD analysis. Each spectrum represents the average of three distinct spectral recordings. The contribution of buffer to the measured ellipiticity was substracted as blank. Molar ellipticity values were calculated using the expression

$$\phi = \frac{\varepsilon}{10\,cnl}$$

where $\varepsilon$ is the ellipticity (millidegrees), $c$ is the protein concentration (moles per liter), $l$ is the cuvette path length, and $n$ is the number of aminoacid residues in the protein. Thermal denaturation/renaturation was performed by heating samples at a constant rate of 1 °C/min, while monitoring the ellipticity at 222 nm. $T_m$ was defined as the temperature at which 50% of protein molecules are unfolded. The amount of secondary structural elements was estimated with the CD-Pro software.

### 2.10. Analytical size-exclusion chromatography

Chromatography analysis was performed using a superdex 200 HR 10/30 column (Amersham Biosciences) equilibrated with KHE running at a flow rate of 1 ml/min at room temperature. MCL-1 was incubated with different amounts of gossypol for 10 min at 37 °C, prior to chromatographic analysis. The column was calibrated with gel-filtration standard proteins from Pharmacia. A 250-μl sample was loaded on to the column and the eluate was monitored at 280 nm.

### 2.11. Monolayer surface pressure measurements

Surface pressure measurements were carried out with a MicroTrough-S system from Kibron (Helsinki, Finland) with constant stirring, at 37 °C. Lipid monolayers were prepared with a lipid composition resembling that of MOM contact sites [(40 PC/35 PE/10 PI/15 CL (mol/mol)] (MOM-like monolayers). The lipid, dissolved in chloroform and methanol (2:1), was gently spread over the surface of 1-ml KHE buffer and kept at a constant surface area. The desired initial surface pressure was attained by changing the amount of lipid applied to the air–water interface. After 10 min to allow for solvent evaporation, compounds of interest were injected through a hole connected to the subphase, and the change in surface pressure was recorded as a function of time until a stable signal was obtained. Under these conditions, maximal surface pressures

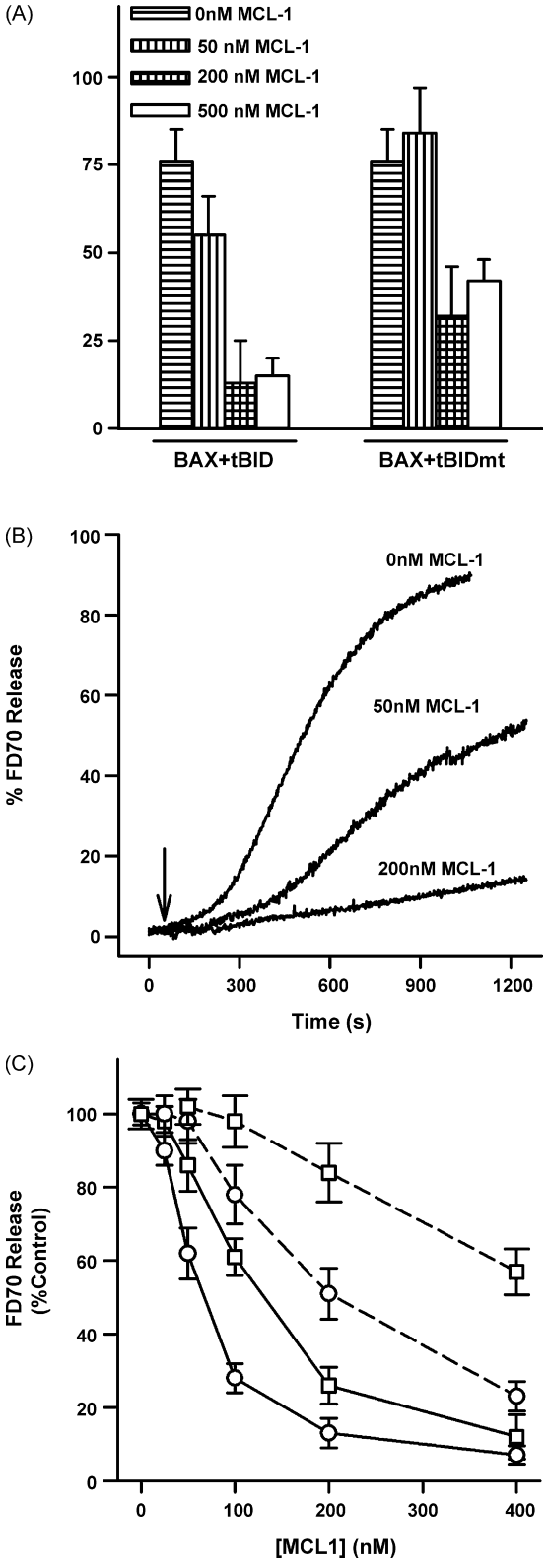


**Fig. 1 – Both MCL-1:tBID and MCL-1:BAX binding interactions contribute to MCL-1-mediated inhibition of BAX permeabilizing function. (A) Effect of different MCL-1 concentrations on the release of mitochondrial cytochrome c induced by BAX (50 nM) combined with either tBID (20 nM) or tBID97A98A (tBID mt, 20 nM). Data represent mean values and standard errors (S.E.) from duplicate experiments. (B) Effect of different MCL-1 concentrations on the release of FD70 from MOM-like LUV induced by BAX (50 nM) combined with tBID (50 nM). Vesicles were treated for 5 min with indicated amounts of MCL-1, prior to addition of proapoptotic proteins (arrow). (C) Dose-dependence of MCL-1-mediated inhibition of vesicular FD70 release induced by BAX plus tBID (circles, continuous line), BAX plus tBID97A98A (circles, dashed line), BAX exposed to 50 °C (squares, continuous line), and BAX exposed to 50 °C plus BAX BH3 peptide (squares, dashed line). Concentration of all proteins was 50 nM, while concentration of BAX BH3 peptide was 2 μM. Data were normalized to a percentage of the release induced by BAX in the absence of MCL-1, representing mean values and standard errors (S.E.) from at least three independent measurements.**

obtained after injecting compounds in the absence of a lipid monolayer were below initial monolayer pressure values examined.

## 3. Results

### 3.1. *Gossypol reverses MCL-1's inhibitory effect on BAX permeabilizing function in a reconstituted liposomal system*

This and other laboratories have shown that the BAX-driven MOMP pathway triggered by tBID can be reconstituted in vitro using recombinant purified proteins and either isolated mitochondria or MOM-like LUV [6]. We first wished to examine the capacity of MCL-1 to inhibit the permeabilizing function of BAX in these in vitro reconstituted systems. To this aim, we obtained the BCL-2-like fold of MCL-1 from *E. coli* in a purified and soluble form (MCL-1ΔN151ΔC23, named MCL-1 hereafter). As previously seen with other antiapoptotic BCL-2 family members [40], recombinant MCL-1 inhibited the release of both cytochrome c and vesicular FD70 elicited by the combination of BAX and tBID in a similar dose-dependent manner (Fig. 1). By contrast, combining MCL-1 with either BAX or tBID alone did not produce significant permeability changes in mitochondrial or liposomal assay systems (Supplementary Fig. 1A). The specificity of MCL-1's inhibitory effect on BAX permeabilizing function was further confirmed by the inability of this antiapoptotic protein to decrease the release of vesicular contents induced by tetanolysin and *S. aureaus* α-toxin, two well-known pore-forming toxins (Supplementary Fig. 1B).

All BCL-2 type proteins examined to date have been shown to contain a well-structured hydrophobic surface, the BH3-binding groove, than can act as a "receptor" for an amphipathic α-helical BH3 "ligand" of pro-apoptotic partners [4,43–46]. However, a controversial issue is whether antiapoptotic proteins inhibit BAX-driven MOMP by binding to and neutralizing BAX itself, "activator" BH3-only proteins such as tBID, or both types of proapoptotic molecules [1–6]. To test whether MCL-1 inhibition of BAX permeabilizing function relies on the interaction between the hydrophobic groove of MCL-1 and the BH3 domain of tBID, a tBID BH3 mutant was used (tBID97A98A) which does not stably interact with MCL-1

but still binds to BAX [5]. Substituting tBID for tBID97A98A substantially decreased but did not abolish the inhibition exerted by MCL-1 on the release of cytochrome c and vesicular FD70 (Fig. 1A and C). These results, together with previous data showing that BID BH3 peptides only partially reverse MCL-1's inhibitory effect on BAX permeabilizing function [40], indicate that sequestration of tBID by MCL-1 is not the only mechanism by which MCL-1 inhibits functional BAX activation.

We recently demonstrated that exposure to moderate heat directly activates BAX permeabilizing function in MOM-like LUV in a manner inhibitable by the complete set of mammalian BCL-2 type proteins [40]. To test whether the inhibition exerted by MCL-1 on the permeabilizing function of heat-activated BAX relies on the interaction between the hydrophobic groove of MCL-1 and the BH3 domain of BAX, we examined whether incubating MCL-1 with a synthetic peptide representing the BAX BH3 domain restores vesicular dextran release. In agreement with this notion, the BAX BH3 peptide markedly diminished the protection conferred by MCL-1 on the permeabilizing function of heat-activated BAX (Fig. 1C), whereas a peptide harbouring mutations known to abolish binding of BH3 ligands to the hydrophobic groove of MCL-1 was virtually ineffective [45] (Supplementary Fig. 1C). In control experiments, minor effects on membrane permeability were observed when vesicles were treated with the BAX BH3 peptide in combination with either heat-activated BAX or MCL-1 alone (Supplementary Fig. 1C).

Having established that the inhibitory function of MCL-1 on BAX permeabilizing activity can be reproduced in MOM-like LUV, we then used this reconstituted liposome system to examine the impact of gossypol on BAX-induced membrane permeabilization. Despite its incapacity to directly affect BAX permeabilizing function, gossypol effectively overrode MCL-1-mediated inhibition of vesicular FD70 release induced by either tBID- or heat-activated BAX (Fig. 2A). In contrast, gossypol had no significant effect on dextran release when MCL-1 was combined with BAX plus $BIM_L$, consistent with previous data indicating that BIM does not function as a direct "activator" of BAX in liposomal and mitochondrial reconstituted systems [40]. As a further measure of specificity, we found that unlike gossypol, epigallocatechin (EGC) and chelerytrine (CHEL), two other polyphenolic compounds derived from plants, did not reverse MCL-1's inhibitory effect of BAX-induced liposome permeabilization (Supplementary Fig. 1D).

BAX and BID often exist as cytosolic proteins in healthy cells, but they translocate to the MOM upon apoptosis triggering to breach this permeability barrier [1]. One mechanism by which BCL-2 type proteins have been shown to inhibit MOMP is by blocking recruitment of these proapoptotic proteins to the MOM. Thus, we decided to examine the association of different BCL-2 family proteins with MOM-like liposomes under conditions reflecting those used in vesicular permeabilization experiments. To this aim, liposomes were incubated with mixtures containing BAX plus tBID with or without MCL-1 and gossypol. Then, liposome-containing and liposome-devoid fractions were separated by centrifugation, and the contents of liposome-bound and free BAX, tBID and MCL-1 were determined by immunoblotting. In correlation

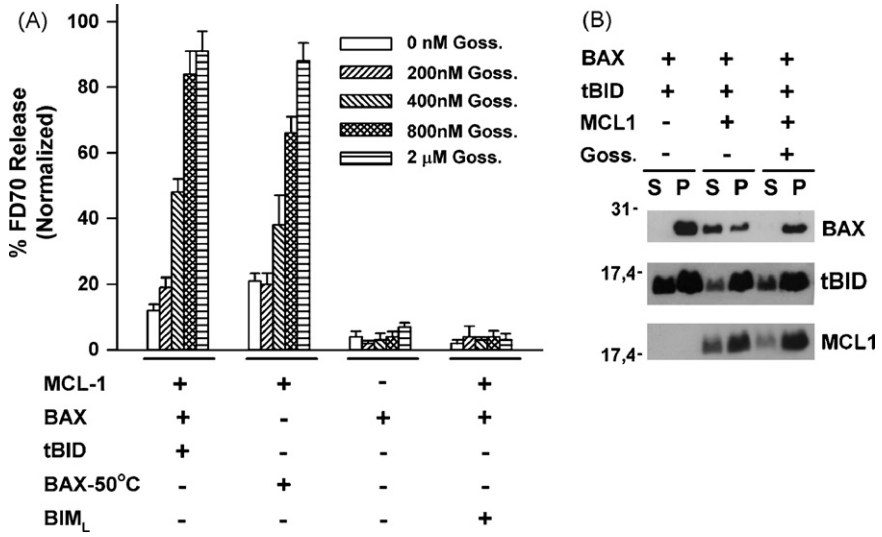


**Fig. 2 – Gossypol reverses the inhibition elicited by MCL-1 on functional BAX activation. (A) Gossypol restores BAX-induced vesicular FD70 release in the presence of inhibitory concentrations of MCL-1. MOM-like LUV were treated with indicated combinations of BCL-2 family proteins and gossypol (Goss.) as explained in Section 2. Extents of vesicular FD70 were normalized to those obtained by a mixture of BAX plus tBID. All proapoptotic proteins were added at 50 nM, while MCL-1 concentration was 200 nM. Data represent mean values and S.E. from 3 to 5 independent measurements. (B) Effect of gossypol on the association of BCL-2 proteins with MOM-like liposomes. Freeze and thawed vesicles were incubated with indicated combinations of BCL-2 family proteins with or without gossypol, followed by centrifugation of reaction mixtures. Equivalent volumes of liposome-free supernatant (S) and liposome-containing pellet (P) fractions were then subjected to SDS-PAGE and anti-BAX, anti-BID or anti-MCL-1 Western-blot analysis. Concentrations of BAX, tBID, MCL-1 and gossypol were 50 nM, 50 nM, 200 nM, and 800 nM, respectively.**

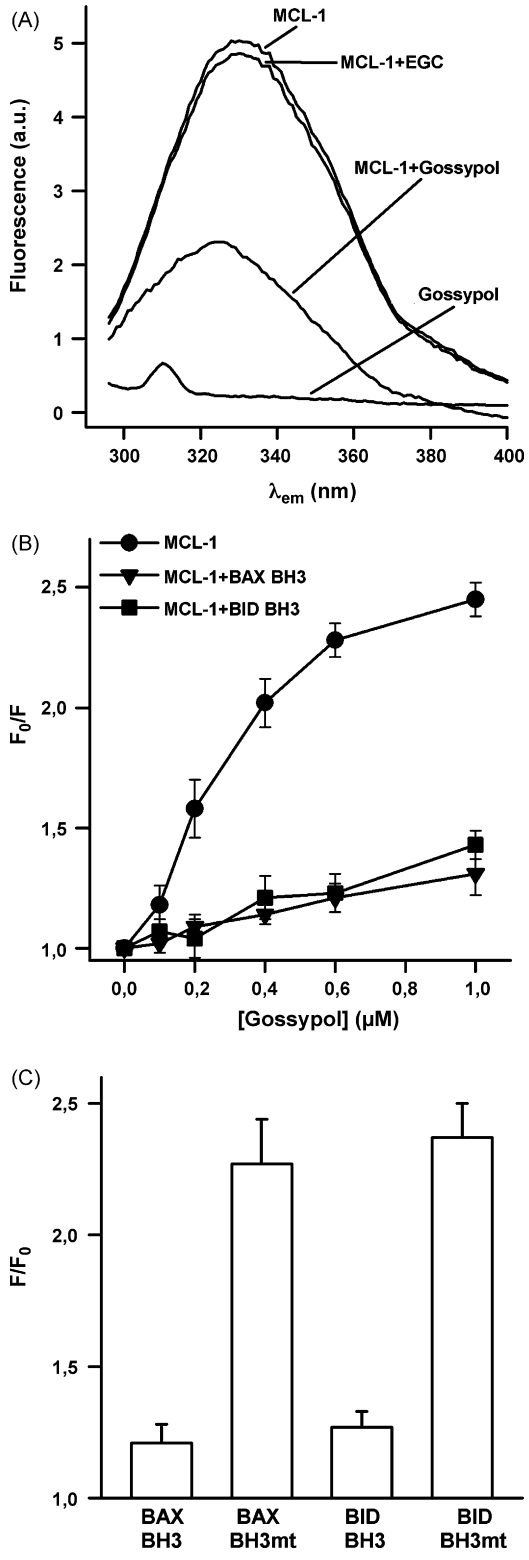


**Fig. 3 – Analysis of gossypol binding to MCL-1 monitored by intrinsic protein fluorescence measurements. (A) Representative tryptophan fluorescence emission spectra of 200 nM MCL-1 alone (MCL-1), 200 nM MCL-1 combined with 2 μM epigallocathecin (MCL-1 + EGC), 200 nM MCL-1 combined with 600 nM gossypol (MCL-1 + gossypol), and 600 nM gossypol alone (gossypol). (B) Dose-dependence of gossypol-induced increase in the tryptophan fluorescence intensity of MCL-1 in the absence or presence of indicated BH3 peptides. MCL-1 and peptide concentrations were 200 nM and 2 μM, respectively. $F_0$, the intensity measured in the absence of gossypol; F, the intensity measured at indicated concentrations of gossypol. Data shown are averages plus S.E. of relative intensities ($F_0$/F) from three independent measurements. (C) Gossypol-induced increase in the tryptophan fluorescence intensity of MCL-1 in the absence or presence of indicated BH3 peptides. MCL-1, gossypol and BH3 peptide concentrations were 200 nM, 600 nM, and 2 μM, respectively. Data shown are averages plus S.E. of relative intensities ($F_0$/F) from duplicated measurements.**

with results obtained in permeabilization assays, MCL-1 markedly decreased the amount of BAX recruited to MOM-like liposomes, while gossypol restored the amount of membrane-bound BAX to the level observed in the absence of MCL-1 (Fig. 2B). On the contrary, gossypol did not affect substantially the association of tBID or MCL-1 with MOM-like liposomes.

In summary, these experiments showed that (i) binding interactions between the hydrophobic groove of MCL-1 and the BH3 domain of both BAX and tBID contribute to inhibition of BAX permeabilizing function by MCL-1; and (ii) at submicromolar concentrations, gossypol effectively disables the capacity of MCL-1 to inhibit functional BAX activation in MOM-like liposomes.

### 3.2. *Gossypol competes in solution with BAX BH3 and BID BH3 peptide ligands for binding to MCL-1*

To further explore the molecular mechanism by which gossypol reverses the inhibitory effect of MCL-1 on functional BAX activation, we switched to solution-based binding studies. MCL-1 possesses three tryptophan residues (W241, W287, and W294) which are buried in a tightly packed hydrophobic interface [43], and all localize within or in close proximity to the interaction region between gossypol and BCL-2/BCL-$X_L$ [31–33]. Based on these observations, we decided to examine whether gossypol affects the tryptophan fluorescence emission spectrum of MCL-1. Free MCL-1 in solution displayed an intrinsic fluorescence emission spectrum with a maximum ($\lambda_{max}$) at 331 nm (Fig. 3A). Upon incubation with gossypol, but not EGC, the $\lambda_{max}$ was blue-shifted to 328 nm with the fluorescence intensity showing a dramatic decrease (Fig. 3A). In contrast, gossypol did not change the fluorescence emission spectrum of MCL-1 in the presence of denaturing concentrations of GuHCl indicating that retention of the tertiary protein fold is required for gossypol:MCL-1 interaction (data not shown). To examine whether gossypol and proapoptotic BH3 ligands compete for the same binding site on MCL-1, the protein was incubated with peptides representing BAX BH3 and BID BH3 domains and then challenged with increasing concentrations of gossypol (Fig. 3B). In concert with this logic, BAX BH3 or BID BH3 peptides virtually eliminated the increase of MCL-1 intrinsic fluorescence intensity elicited by gossypol, while peptides containing mutations known to be

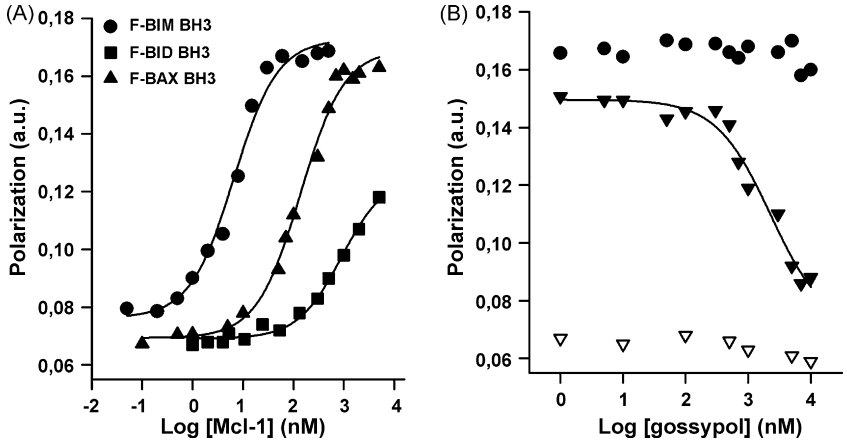


**Fig. 4 – Analysis of gossypol binding to MCL-1 monitored by fluorescence polarization (FP) measurements. (A) FP analysis of MCL-1 binding to F-BIM BH3, F-BID BH3 and F-BAX BH3 peptides. Various concentrations of MCL-1 were incubated with a fixed concentration of indicated BH3 peptides (5 nM) for 30 min, followed by determination of FP. Data represent mean ($n$ = 3), with S.E. being ≤15% in all cases. (B) Gossypol competes with F-BAX BH3 peptide for binding MCL-1. MCL-1 (400 nM) was pre-incubated with indicated concentrations of gossypol for 10 min, before adding 5 nM F-BAX BH3 (closed triangles) or F-BIM BH3 (closed circles) peptides (5 nM). FP was measured after 30 min. Open triangles represent control experiments showing that gossypol does not interfere with fluorescence polarization signal of F-BAX BH3 peptide alone. Data represent mean ($n$ = 3), with S.E. being ≤10% in all cases.**

**Table 1 – Mean $EC_{50}$ (nM) values obtained for binding reactions between selected F-BH3 peptides and BCL-2 family proteins**

| Protein/peptide | F-BIM BH3 | F-BID BH3 | F-BAX BH3 |
|---|---|---|---|
| MCL-1 | 11.2 | 2340.5 | 143.4 |
| BAX | >50000 | >50000 | >50000 |

critical for BH3 ligand binding to MCL-1's hydrophobic groove were without effect [44] (Fig. 3C).

To confirm by an independent method the ability of gossypol to compete with BH3 peptide ligands for binding to the hydrophobic groove on MCL-1, fluorescence polarization (FP) assays were used. First, various concentrations of MCL-1 were titrated into reactions containing a fixed concentration of F-BAX BH3, F-BID BH3, or F-BIM BH3 peptides. As shown in Fig. 4A, FP-based assays indicated that F-BIM BH3 and F-BAX BH3 peptides bound to MCL-1 in a concentration-dependent and saturable manner within the nanomolar range, whereas F-BID BH3 peptide bound MCL-1 with lower affinity (Fig. 4A). The relative MCL-1 binding affinities ($EC_{50}$) of F-BIM BH3, F-BAX BH3, and F-BID BH3 peptides were 11.2, 143.4, and 2140.5 nM, respectively (Table 1). This is consistent with previous studies indicating that BIM BH3 binds more tightly to MCL-1 hydrophobic groove than BAX BH3 and BID BH3 ligands [47]. Since a 34-mer BID BH3 peptide containing BH3-flanking regions reportedly binds to the hydrophobic groove MCL-1 with nanomolar affinity [5,45], the low (micromolar) binding affinity of our F-BID BH3 peptide may be due to its relatively short length. On the other hand, none of the three F-BH3 peptides bound detectably to BAX up to a concentration of 50 μM, presumably due to the presence of a C-terminal hydrophobic helix in BAX which folds intramolecularly occupying its hydrophobic groove [1] (Table 1).

Next, we evaluated the ability of gossypol to compete with F-BAX BH3 and F-BIM BH3 peptides in binding to MCL-1.

**Table 2 – Effect of different gossypol/MCL-1 ratios (mol/mol) on various structural and lipid-interacting properties of MCL-1**

| | Gossypol/MCL-1 (0/1) | Gossypol/MCL-1 (1/1) | Gossypol/MCL-1 (3/1) |
|---|---|---|---|
| Helicity (%)[a] | 67.1 ± 2.4 | 65.1 ± 3.1 | 65.5 ± 2.4 |
| $T_m$ (°C) | 74.1 ± 1.8 | 73.5 ± 2.2 | 73.9 ± 2.5 |
| $m_G$ (Kcal/mol/M) | 5.4 ± 0.5 | N.D. | 5.8 ± 0.4 |
| $\Delta G°(H_2O)$(Kcal/mol) | 12.1 ± 1.3 | N.D. | 11.6 ± 1.5 |
| Mol. weight (KDa) | 18.6 | 18.5 | 18.3 |
| Protein bound (%) | 65.3 ± 5.6 | 68.3 ± 4.2 | 63.1 ± 6.2 |
| Critical pressure | 29.2 mN/m | 30.8 mN/m | N.D. |
| Release, pH 5.5 (%) | 65.2 ± 6.1 | 56.3 ± 8.3 | 60.2 ± 7.6 |

[a] Procedures used for analyzing different properties of MCL-1 explained in Section 2. All data correspond to mean values plus S.E. obtained from at least two independent measurements, except for estimated molecular weight (mol. weight) and critical pressure values which correspond to single measurements. N.D.: Not determined.

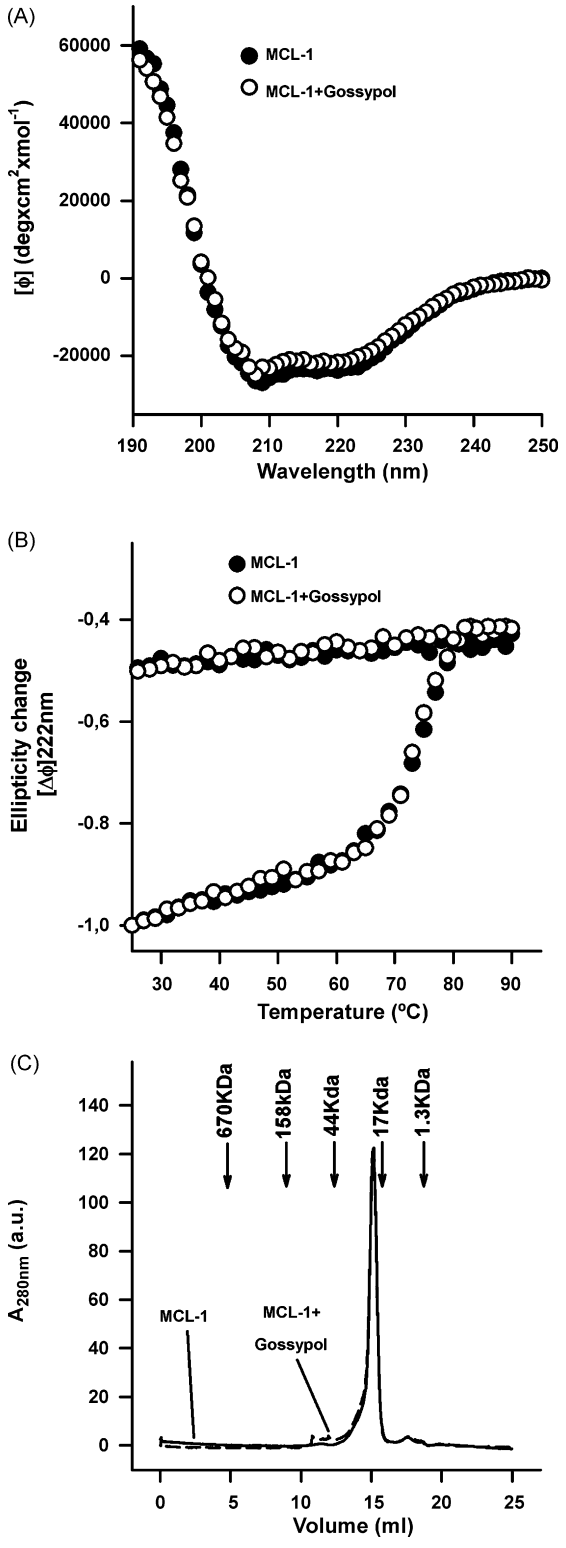


**Fig. 5 – Gossypol binding produces minor structural changes to MCL-1. (A) CD spectrum of MCL-1 in the absence (MCL-1) or presence of gossypol (MCL-1 + Gossypol). MCL-1 and gossypol concentrations were 5 μM. (B) Thermal denaturation curves for MCL-1 in the absence (MCL-1) or presence of gossypol (MCL-1 + Gossypol). MCL-1 and gossypol concentrations were 5 μM. Thermal denaturation curves were obtained by recording the temperature dependence of MCL-1 ellipticity at 222 nm. Temperature scans were performed at a heating or cooling rate of 1 °C/min. Ellipticity was measured from 25 °C to 95 °C (lower data points) and then back to 25 °C (higher data points) to assess the reversibility of denaturation. The molar ellipticity at 25 °C was set to −1 to compare the thermal denaturation rates. (C) Representative chromatograms of 10 μM MCL-1 in the absence (continuous line) or presence of 10 μM gossypol (discontinuous line). Arrows indicate elution profiles or protein standards of known molecular weights.**

FP-based assays determined that gossypol competes with F-BAX BH3 for binding MCL-1 with an estimated $IC_{50}$ of 1.84 μM, while up to 10 μM concentrations of gossypol did not affect binding of F-BIM BH3 to MCL-1 (Table 2). Incubating gossypol with F-BAX BH3 peptide in the absence of MCL-1 only marginally affected background fluorescence polarization, excluding a direct effect of gossypol on the peptide probe as an explanation for results obtained (Fig. 4B).

In short, solution-based assays supported the notion that gossypol reverses MCL-1's inhibitory effect on BAX permeabilizing function by competing with both BAX BH3 and BID BH3 ligands for binding to the hydrophobic groove of MCL-1.

### 3.3. *Gossypol neither produces major changes in MCL-1 structural properties nor converts MCL-1 into a BAX-like pore-forming molecule*

In a previous study, a model was proposed whereby gossypol docking into the hydrophobic groove of BCL-2 produces a conformational change in this protein that unleashes a latent BAX-like pore-forming activity [33]. Thus, we next investigated this potential mode of gossypol action for the case of MCL-1. First, we examined whether interaction with gossypol leads to detectable changes in MCL-1 secondary structure, as assessed by far-UV CD spectroscopy. As expected, the far-UV CD spectrum of MCL-1 revealed absorption minima at 208 nm and 222 nm characteristic of helical proteins (Fig. 5A). Analysis of the secondary structure composition of MCL-1 indicated 67.1% α-helical, 3.8% β-sheet, 6.6% turns, and 22.5% unordered content, in agreement with structural data obtained by NMR (Table 2) [43]. Upon incubation with gossypol, however, minimal changes were observed in the overall CD spectrum of MCL-1, as well as in the estimated helical content of the protein (Fig. 5A, and Table 2).

To investigate putative changes produced by gossypol on the tertiary structure of MCL-1, the conformational stability of the protein was analyzed by thermal denaturation assays. Unfolding and refolding of MCL-1 were monitored by the change in ellipticity at 222 nm as a function of temperature (Fig. 5B). The thermal unfolding curve showed a sharp transition suggesting a two-state mechanism, although other mechanisms are not excluded. Denaturation was not reversible under conditions studied. The estimated melting temperature ($T_m$), for MCL-1 was 74.1 °C consistent with the compact globular fold, resembling a single folding unit, described by NMR. Importantly, gossypol only produced slight changes in MCL-1 melting curve and $T_m$ (Fig. 5B and Table 2). To further examine the effect of gossypol on MCL-1 conformational stability under conditions more closely reflecting

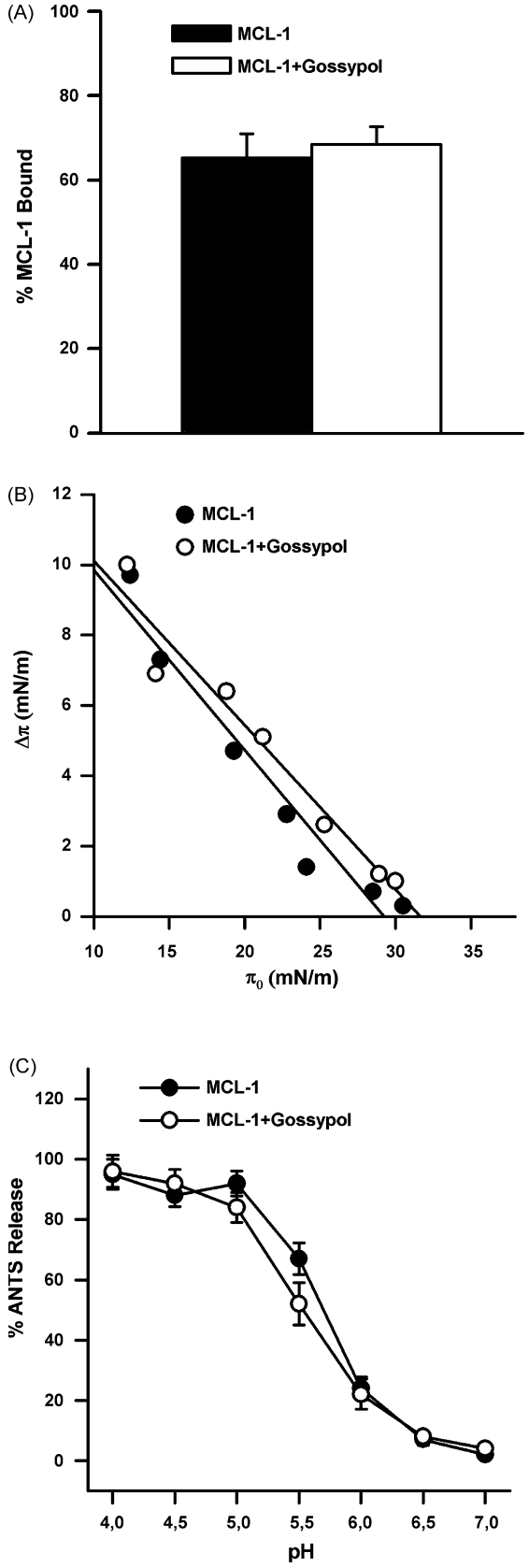


**Fig. 6 – Gossypol binding produces minor changes to lipid-interacting properties of MCL-1. (A) Effect of gossypol on the association of MCL-1 with MOM-like liposomes. Freeze-thawed MOM-like liposomes containing brominated lipids and indicated compounds were incubated overnight at 37 °C, followed by sedimentation of lipid vesicles by centrifugation, and quantitation of liposome-associated protein fraction. The data are means of at least three independent measurements. (B) Effect of gossypol on the penetration of MCL-1 into MOM-like lipid monolayers. Changes in monolayer surface pressure ($\Delta\pi$) elicited by addition of MCL-1 alone (MCL-1) or MCL-1 plus gossypol (MCL-1 + gossypol) to the subphase, measured as function of the initial surface pressure ($\Delta\pi$). MCL-1 and gossypol concentrations were 200 nM. The data are fit to a straight line, and the *x*-intercepts correspond to the monolayer critical surface pressure ($\pi_c$), which provides a measure of the membrane penetrability of the protein. (C) Effect of gossypol on the release of vesicular ANTS/DPX induced by MCL-1 at different pHs. The concentration of MCL-1 and gossypol was 200 nM. Extents of dye release are representative of 3–6 independent measurements. In all cases, MCL-1 was incubated with gossypol for 5 min prior to analysis of interaction with model membrane systems.**

those used in vesicle permeabilization and solution-based binding assays, chemical denaturation experiments were performed. Here, the intrinsic fluorescence emission maximum of MCL-1 was monitored at 37 °C as a function of increasing GuHCl concentrations, in KHE buffer with or without gossypol, and using submicromolar dosing of MCL-1 and gossypol (Supplementary Fig. 2). Analysis of the data using a two-state model did not detect major changes in the free energy of MCL-1 unfolding upon incubating the protein with gossypol under these assay conditions (Table 2).

A number of BCL-2 family members have been shown to shift from a monomeric to an oligomeric form upon different treatments, raising the possibility that interaction with gossypol may trigger a monomer-to-oligomer shift in MCL-1. To address this, we incubated MCL-1 with various amounts of gossypol and performed size-exclusion chromatography analysis of the samples. MCL-1 exhibited nearly identical elution profiles in all cases analyzed, with molecular weight estimates being close to the actual molecular weight of monomeric MCL-1, as determined using calibration curves with protein standards of known molecular weights (Fig. 5C, Table 2).

We next examined the putative impact of gossypol on various lipid-interacting properties of MCL-1. First, we tested whether MCL-1 by itself is able to bind to MOM-like liposomes using an assay that allows determining liposome association of an individual protein in a quantitative manner [42]. As seen in Fig. 6A, upon incubation with MOM-like liposomes a large fraction of MCL-1 associated to the liposomes, while addition of gossypol did not produce substantial changes in the liposome-binding capacity of MCL-1.

Next, we compared changes in the surface pressure of MOM-like monolayers elicited by MCL-1 alone or in combination with gossypol. In these experiments, the increase in surface pressure upon protein addition was measured, $\Delta\pi$, as a function of the initial surface pressure, $\pi_0$. As the initial surface pressure is increased, the change in surface pressure

upon protein addition decreased, as expected (Fig. 6B). The data fit well to a straight line giving a critical surface pressure ($\pi_c$) of 29.2 mN/m for MCL-1. The critical surface pressure is a measure of the penetration capacity of a protein entering a lipid monolayer. The changes in monolayer surface pressure observed upon addition of MCL-1 combined with gossypol also decreased as a function of increasing initial surface pressure, giving a $\pi_c$ value somewhat higher than that obtained with the protein alone (30. 8 mN/m, Table 2). Because the pressure estimated for a membrane bilayer is >32 mN/m [48], we infer from these results that MCL-1 does not penetrate into the hydrophobic matrix of the lipid bilayer, irrespective of the absence or presence of gossypol.

Finally, we addressed whether MCL-1 might affect membrane integrity in a gossypol-regulated manner, by examining the capacity of this protein to release a small fluorescent dye (ANTS) encapsulated inside MOM-like LUV as a function of pH. MCL-1 produced little change in ANTS fluorescence at neutral pH, but decreasing the pH of the solution to acidic values progressively augmented the ability of MCL-1 to induce vesicular ANTS release (Fig. 6C). As seen with other lipid-interacting parameters, gossypol did not modify substantially the pH-dependence of MCL-1-induced vesicular ANTS release (Fig. 6C, and Table 2).

Altogether, these results strongly suggest that complexation with gossypol does not produce major changes in structural or lipid-interacting properties of MCL-1, at least under experimental conditions used in our reconstitution assays.

## 4. Discussion

MCL-1 is an important survival factor both for healthy and malignant cells [1]. Thus, great interest exists in understanding the exact mechanism of MCL-1 action and in developing new strategies that inactivate its prosurvival function. However, the study of MCL-1 protein action in intact cells is not easy. A major problem is that MCL-1 is a short-lived protein which seems to be dynamically regulated by a wide array of cellular processes. In addition, the likely site of MCL-1 action (i.e. the MOM) is also a complicating factor, since membrane proteins can be made to reveal their secrets only with difficulty. In an attempt to circumvent these problems, we used simplified systems amenable for detailed mechanistic studies to advance in our understanding of the antiapoptotic mode of MCL-1 action, as well as to gain more insight into how gossypol influences MCL-1 function at the molecular level.

Exactly how protein–protein interactions among BCL-2 family members modulate apoptosis is the subject of ongoing debate [1–3,5,6]. Two major competing models have been proposed. On the one hand, the ''direct'' model (''indirect'' model from the perspective of BH3-only proteins) postulates that BCL-2-type proteins engage BAX-type proteins in non-productive interactions via their BH3-binding groove. In turn, binding of BH3-only proteins to anti-apoptotic partners unleashes BAX-type proteins, which then auto-activate to elicit MOMP. On the other hand, the ''indirect'' model (''direct'' model from the perspective of BH3-only proteins) posits that BCL-2-type proteins inhibit MOMP by sequestering a selected subset of ''activator'' BH3-only proteins including tBID and BIM, rather than BAX-type proteins. In this view, docking of so-called ''sensitizer'' BH3-only proteins into the hydrophobic groove of BCL-2 type proteins sets tBID/BIM free to interact with and functionally activate BAX-type proteins.

Our results do not comply with either of the two aforementioned models in that we found that physical interaction of MCL-1 with *both* BAX and tBID contributes to MCL-1's inhibitory effect on BAX permeabilizing function. On the other hand, the findings reported here for the antiapoptotic mode of MCL-1 action are in accord with a recently promulgated model for BCL-$X_L$, in which both BCL-$X_L$:BAX and BCL-$X_L$:tBID interactions were found relevant for inhibition of BAX permeabilizing function by BCL-$X_L$ [49]. Moreover, we recently reported that in addition to MCL-1, BCL-$X_L$, BCL-2, BCL-W and A1 also inhibit the permeabilizing function of tBID- or heat-activated BAX in MOM-like liposomes [40]. Collectively, these observations lead us to propose that the ''dual-interaction'' model reflects a common antiapoptotic mode of action shared by all BCL-2 type proteins. In addition, other types of interactions with cellular factors outside the BCL-2 family are also likely to contribute to the antiapoptotic function BCL-2 type proteins [6,50].

The BAX-induced membrane permeabilization process can be dissected into several major steps, including translocation of BAX to the membrane, intramembranous BAX oligomerization, and opening/expansion of a proteolipidic pore [6]. Because MCL-1 clearly decreased the amount of BAX bound to MOM-like liposomes, MCL-1 appears to act, at least in part, by blocking the earliest step in the process leading to membrane permeabilization (i.e. BAX translocation to the membrane). On the other hand, the finding that MCL-1 does not reduce the amount of tBID bound to the liposomes could be explained by the presence in tBID of a cardiolipin-binding domain allowing this protein to target these vesicles via protein–lipid interactions [40]. Since the outcome of MCL-1:BAX and MCL:tBID interactions is not the same, MCL-1 seems to utilize multiple mechanisms to inhibit functional BAX activation via interactions with BAX and tBID, as recently proposed for BCL-$X_L$ [49]. Furthermore, as in the case of BCL-$X_L$, MCL-1 was found to be largely membrane-associated under conditions inhibiting functional BAX activation in our reconstituted liposomal system. Interestingly, recruitment of MCL-1 to MOM-like liposomes did not require the presence of a hydrophopic region present at the C-terminus of BCL-2 type proteins, and occurred independently of BAX and tBID. One possible explanation for this phenomenon is that regions of positive electrostatic potential present in MCL-1 may allow this protein to associate with the negatively-charged surface of MOM-like vesicles [43]. We are currently investigating this possibility.

Previous studies showed that gossypol and its derivatives can bind to the hydrophobic groove of BCL-2/BCL-$X_L$/MCL-1 in such a manner as to displace BID BH3 and BIM BH3 ligands, leading to the proposal that these compounds promote BAX-driven MOMP by unsequestering ''activator'' BH3-only proteins from antiapoptotic BCL-2 type proteins [31,32,34]. In this regard, we now report the following novel findings: (a) gossypol effectively competes not only with BID BH3 but also with BAX BH3 ligand for binding to the hydrophobic groove of

MCL-1, and (b) gossypol reverses the inhibition exerted by membrane-associated MCL-1 on BAX permeabilizing function, not only in the presence of tBID but also in the absence of any BH3-only protein. In combination, these observations support a model whereby gossypol docking into the BH3-binding groove of MCL-1 unleashes *both* BAX "activator" molecules such as tBID as well as BAX itself, thereby effectively promoting membrane permeabilization. This effect resembles that observed with BIM and BIM BH3 peptides in MOM-like liposomes [40]. However, our results do not imply that gossypol is strictly a functional mimetic of BIM or its BH3 domain when triggering apoptosis, since gossypol does not share with BIM/BIM BH3 the ability to neutralize the complete set of antiapoptotic proteins at low nanomolar concentrations [34,40,47]. Moreover, emerging evidence indicates that regions outside the BH3 domain can contribute to the proapoptotic function of BH3-only proteins such as BIM and tBID [51]. As a prominent example, the cardiolipin-binding domain of tBID has been shown to potentiate BAX-induced membrane permeabilization and to promote activation of a variety of apoptosis-related mitochondrial proteins [40,52–55]. Although it is clear that gossypol differs from tBID in that it does not directly activate BAX permeabilizing function, it remains to be formally tested whether this compound may exert some of its cytotoxic effects by interaction with mitochondrial membrane lipids.

Under certain settings, BCL-2 type proteins change conformation to become pro-apoptotic factors that induce, rather than inhibit MOMP [6]. Indeed, we previously showed that cleavage by caspases unleashes a latent BAX-like pore-forming activity in BCL-$X_L$ [41]. In line with this, Lei et al. reported that gossypol binding to the BH3-binding groove of BCL-2 transforms this protein into a BAX-like molecule capable of forming cytochrome *c*-transporting pores in isolated mitochondria and in pure lipid vesicles [33]. However, we found no evidence indicating that gossypol binding produces substantial changes on MCL-1's structural or lipid-interacting properties. Considering that the BH3-binding grooves of BCL-2 and MCL-1 are significantly different [43–45], one possible explanation for this apparent discrepancy is that complexation with gossypol does not lead to the same conformational changes in BCL-2 and MCL-1. On the other hand, we note that activation of a BAX-like permeabilizing function in BCL-2 required concentrations of gossypol ~100-fold higher than the ones we used here with MCL-1 [33]. Hence, an alternative explanation is that gossypol similarly influences BCL-2 and MCL-1 function via a dual concentration-dependent effect, as follows: (a) at relatively low (submicromolar) concentrations, gossypol untethers proapoptotic BCL-2 family members from BCL-2 and MCL-1, and (b) above a certain treshold, gossypol unleashes a BAX-like pore-forming activity that is normally latent in both BCL-2 and MCL-1. In future studies with in vitro reconstituted systems, it would be particularly instructive to comparatively examine how increasing doses of gossypol influence the behavior of different BCL-2 family members in their membrane-associated forms. Irrespective of the outcome of such mechanistic studies, the finding reported here that gossypol reverses MCL-1-medited inhibition of functional BAX activation implies that this compound and its derivatives may be effective eliminating barriers to apoptosis induction by ABT-737 and conventional chemotherapeutic agents in selected cancer cells overexpressing MCL-1.

## Acknowledgements

We thank David Huang (The Walter and Eliza Hall Institute of Medical Research, Parkville, Australia) for providing plasmids for expression of recombinant MCL-1. This work was supported by Ministerio de Ciencia y Tecnologia Grant BFU2005-06095. A.E. is a recipient of a predoctoral fellowship from the Basque Government.

## Appendix A. Supplementary data

Supplementary data associated with this article can be found, in the online version, at doi:10.1016/j.bcp.2008.08.003.

## REFERENCES

[1] Youle RJ, Strasser A. The BCL-2 protein family: opposing activities that mediate cell death. Nat Rev Mol Cell Biol 2008;9:47–59.
[2] Chipuk JE, Green DR. How do BCL-2 proteins induce mitochondrial outer membrane permeabilization? Trends Cell Biol 2008;18:157–64.
[3] Letai AG. Diagnosing and exploiting cancer's addiction to blocks in apoptosis. Nat Rev Cancer 2008;8:121–32.
[4] Petros AM, Olejniczak ET, Fesik SW. Structural biology of the Bcl-2 family of proteins. Biochim Biophys Acta 2004;1644:83–94.
[5] Willis SN, Fletcher JI, Kaufmann T, van Delft MF, Chen L, Czabotar PE, et al. Apoptosis initiated when BH3 ligands engage multiple Bcl-2 homologs, not Bax or Bak. Science 2007;315:856–9.
[6] Basañez G, Hardwick JM. Unravelling the Bcl-2 apoptosis code with a simple model system. PLoS Biol 2008;6:e154.
[7] Labi V, Grespi F, Baumgartner F, Villunger A. Targeting the Bcl-2-regulated apoptosis pathway by BH3 mimetics: a breakthrough in anticancer therapy? Cell Death Differ 2008;15:977–87.
[8] Oltersdorf T, Elmore SW, Shoemaker AR, Armstrong RC, Augeri DJ, Belli BA, et al. An inhibitor of Bcl-2 family proteins induces regression of solid tumours. Nature 2005;435:677–81.
[9] Chauhan D, Velankar M, Brahmandam M, Hideshima T, Podar K, Richardson P, et al. A novel Bcl-2/Bcl-X(L)/Bcl-w inhibitor ABT-737 as therapy in multiple myeloma. Oncogene 2007;26:2374–80.
[10] Trudel S, Stewart AK, Li Z, Shu Y, Liang SB, Trieu Y, et al. The Bcl-2 family protein inhibitor, ABT-737, has substantial antimyeloma activity and shows synergistic effect with dexamethasone and melphalan. Clin Cancer Res 2007;13:621–9.
[11] Kang MH, Kang YH, Szymanska B, Wilczynska-Kalak U, Sheard MA, Harned TM, et al. Activity of vincristine, L-ASP, and dexamethasone against acute lymphoblastic leukemia is enhanced by the BH3-mimetic ABT-737 in vitro and in vivo. Blood 2007;110:2057–66.
[12] Witham J, Valenti MR, De-Haven-Brandon AK, Vidot S, Eccles SA, Kaye SB, et al. The Bcl-2/Bcl-XL family inhibitor

ABT-737 sensitizes ovarian cancer cells to carboplatin. Clin Cancer Res 2007;13:7191–8.
[13] Kuroda J, Kimura S, Strasser A, Andreeff M, O'Reilly LA, Ashihara E, et al. Apoptosis-based dual molecular targeting by INNO-406, a second-generation Bcr-Abl inhibitor, and ABT-737, an inhibitor of antiapoptotic Bcl-2 proteins, against Bcr-Abl-positive leukemia. Cell Death Differ 2007;14:1667–77.
[14] Del Gaizo Moore V, Schlis KD, Sallan SE, Armstrong SA, Letai A. BCL-2 dependence and ABT-737 sensitivity in acute lymphoblastic leukemia. Blood 2008;111:2300–9.
[15] Kuroda J, Kimura S, Andreeff M, Ashihara E, Kamitsuji Y, Yokota A, et al. ABT-737 is a useful component of combinatory chemotherapies for chronic myeloid leukaemias with diverse drug-resistance mechanisms. Br J Haematol 2008;140:181–90.
[16] Hann CL, Daniel VC, Sugar EA, Dobromilskaya I, Murphy SC, Cope L, et al. Therapeutic efficacy of ABT-737, a selective inhibitor of BCL-2, in small cell lung cancer. Cancer Res 2008;68:2321–8.
[17] van Delft MF, Wei AH, Mason KD, Vandenberg CJ, Chen L, Czabotar PE, et al. The BH3 mimetic ABT-737 targets selective Bcl-2 proteins and efficiently induces apoptosis via Bak/Bax if Mcl-1 is neutralized. Cancer Cell 2006;10: 389–99.
[18] Konopleva M, Contractor R, Tsao T, Samudio I, Ruvolo PP, Kitada S, et al. Mechanisms of apoptosis sensitivity and resistance to the BH3 mimetic ABT-737 in acute myeloid leukemia. Cancer Cell 2006;10:375–88.
[19] Lin X, Morgan-Lappe S, Huang X, Li L, Zakula DM, Vernetti LA, et al. 'Seed' analysis of off-target siRNAs reveals an essential role of Mcl-1 in resistance to the small-molecule Bcl-2/Bcl-XL inhibitor ABT-737. Oncogene 2007;26:3972–9.
[20] Tahir SK, Yang X, Anderson MG, Morgan-Lappe SE, Sarthy AV, Chen J, et al. Influence of Bcl-2 family members on the cellular response of small-cell lung cancer cell lines to ABT-737. Cancer Res 2007;67:1176–83.
[21] Chen S, Dai Y, Harada H, Dent P, Grant S. Mcl-1 down-regulation potentiates ABT-737 lethality by cooperatively inducing Bak activation and Bax translocation. Cancer Res 2007;67:782–91.
[22] Huang F, Sinikrope FA. BH3 mimetic ABT-737 potentiates TRAIL-mediated apoptotic signaling by unsequestering Bim and Bak in human pancreatic cancer cells. Cancer Res 2008;68:2944–51.
[23] Kaufmann SH, Karp JE, Svingen PA, Krajewski S, Burke PJ, Gore SD, et al. Elevated expression of the apoptotic regulator Mcl-1 at the time of leukemic relapse. Blood 1998;91:991–1000.
[24] Kitada S, Andersen J, Akar S, Zapata JM, Takayama S, Krajewski S, et al. Expression of apoptosis-regulating proteins in chronic lymphocytic leukemia: correlations with In vitro and In vivo chemoresponses. Blood 1998;91:3379–89.
[25] Song L, Coppola D, Livingston S, Cress D, Haura EB. Mcl-1 regulates survival and sensitivity to diverse apoptotic stimuli in human non-small cell lung cancer cells. Cancer Biol Ther 2005;4:267–76.
[26] Wuillème-Toumi S, Robillard N, Gomez P, Moreau P, Le Gouill S, Avet-Loiseau H, et al. Mcl-1 is overexpressed in multiple myeloma and associated with relapse and shorter survival. Leukemia 2005;19:1248–52.
[27] Qin JZ, Xin H, Sitailo LA, Denning MF, Nickoloff BJ. Enhanced killing of melanoma cells by simultaneously targeting Mcl-1 and NOXA. Cancer Res 2006;66:9636–45.
[28] Sieghart W, Losert D, Strommer S, Cejka D, Schmid K, Rasoul-Rockenschaub S, et al. Mcl-1 overexpression in hepatocellular carcinoma: a potential target for antisense therapy. J Hepatol 2006;44:151–7.
[29] Cavarretta IT, Neuwirt H, Untergasser G, Moser PL, Zaki MH, Steiner H, Rumpold H, et al. The antiapoptotic effect of IL-6 autocrine loop in a cellular model of advanced prostate cancer is mediated by Mcl-1. Oncogene 2007;26:2822–32.
[30] Pepper C, Lin TT, Pratt G, Hewamana S, Brennan P, Hiller L, et al. Mcl-1 expression has in vitro and in vivo significance in chronic lymphocytic leukemia and is associated with other poor prognostic markers. Blood 2008 July 3 [Epub ahead of print].
[31] Kitada S, Leone M, Sareth S, Zhai D, Reed J, Pellechia M. Discovery, characterization and structure-activity relationships studies of proapoptotic polyphenols targeting B-cell lymphocyte/leukaemia 2 proteins. J Med Chem 2003;46:4259–64.
[32] Wang G, Nikolavska-Coleska Z, Yang CY, Wang R, Tang G, Guo J, et al. Structure-based design of potent small-molecule inhibitors of antiapoptotic Bcl-2 proteins. J Med Chem 2006;49:6139–42.
[33] Lei X, Chen Y, Du G, Yu W, Wang X, Qu H, et al. Gossypol induces Bax/bak-independent activation of apoptosis and cytochrome c release via a conformational change in Bcl-2. FASEB J 2006;20:2147–9.
[34] Zhai D, Jin C, Satterwhait AC, Reed JC. Comparison of chemical inhibitors of antiapoptotic Bcl-2-family proteins. Cell Death Differ 2006;1–3.
[35] Meng Y, Li Y, Li J, Li H, Fu J, Liu Y, et al. (−)Gossypol and its combination with imatinib induce apoptosis in human chronic myeloid leukemic cells. Leuk Lymphoma 2007;48:2204–12.
[36] Kline MP, Rajkumar SV, Timm MM, Kimlinger TK, Haug JL, Lust JA, et al. R-(−)-gossypol (AT-101) activates programmed cell death in multiple myeloma cells. Exp Hematol 2008;36:568–76.
[37] Kitada S, Kress CL, Krajewska M, Jia L, Pellecchia M, Reed JC. Bcl-2 antagonist apogossypol (NSC736630) displays single-agent activity in Bcl-2-transgenic mice and has superior efficacy with less toxicity compared with gossypol (NSC19048). Blood 2008;111:3211–9.
[38] Meng Y, Tang W, Dai Y, Wu X, Liu M, Ji Q, et al. Natural BH3 mimetic (−)-gossypol chemosensitizes human prostate cancer via Bcl-xL inhibition accompanied by increase of Puma and Noxa. Mol Cancer Ther 2008;7:2192–202.
[39] Balakrishnan K, Wierda WG, Keating MJ, Gandhi V. Gossypol, a BH3 mimetic, induces apoptosis in chronic lymphocytic leukemia cells. Blood 2008 Jun 19 [ahead of print].
[40] Terrones O, Etxebarria A, Landajuela A, Landeta O, Antonsson B, Basañez G. BIM and tBID are not mechanistically equivalent when assisting BAX to permeabilize bilayer membranes. J Biol Chem 2008;283:7790–803.
[41] Basañez G, Zhang J, Chau BN, Maksaev GI, Frolov VA, et al. Pro-apoptotic cleavage products of Bcl-xL form cytochrome c-conducting pores in pure lipid membranes. J Biol Chem 2001;276:31083–91.
[42] Thuduppathy GR, Craig JW, Kholodenko V, Schon A, Hill RB. Evidence that membrane insertion of the cytosolic domain of Bcl-$x_L$ is governed by an electrostatic mechanism. J Mol Biol 2005;359:1045–58.
[43] Day CL, Chen L, Richardson SJ, Harrison PJ, Huang DCS, Hinds M. Solution structure of prosurvival Mcl-1 and characterization of its binding by proapoptotic BH3-only ligands. J Biol Chem 2005;280:4738–44.
[44] Czabotar PE, Lee EF, van Delft MF, Day CL, Smith BJ, Huang DC, et al. Structural insights into the degradation of Mcl-1 induced by BH3 domains. Proc Natl Acad Sci USA 2007;104:6217–22.
[45] Day CL, Smits C, Fan FC, Lee EF, Fairlie WD, Hinds MG. Structure of the BH3 domains from the p53-inducible BH3-

only proteins Noxa and Puma in complex with Mcl-1. J Mol Biol 2008;380:958–71.
[46] Smits C, Czabotar PE, Hinds MG, Day CL. Structural plasticity underpins promiscuous binding of the prosurvival protein A1. Structure 2008;16:818–29.
[47] Chen L, Willis SN, Wei A, Smith BJ, Fletcher JI, Hinds MG, et al. Differential targeting of prosurvival Bcl-2 proteins by their BH3-only ligands allows complementary apoptotic function. Mol Cell 2005;17:393–403.
[48] Kimelberg HK, Papahadjopoulos D. Phospholipid-protein interactions: membrane permeability correlated with monolayer ''penetration''. Biochim Biophys Acta 1971;233:805–9.
[49] Billen LP, Kokoski CL, Lovell JF, Leber B, Andrews DW. Bcl-XL inhibits membrane permeabilization by competing with Bax. PLoS Biol 2008;6:e147. doi: 10.1371/journal.pbio.0060147.
[50] Rong YP, Aromolaran AS, Bultynck G, Zhong F, Li X, McColl K, et al. Targeting Bcl-2-IP3 receptor interaction to reverse Bcl-2′s inhibition of apoptotic calcium signals. Mol Cell 2008;31:255–65.
[51] Buck I, Cerella C, Cristofanon S, Reuter S, Diederich M. Novel job opportunities in cell death! Biochem Pharmacol 2008 26 June [ahead of print].
[52] Liu J, Weiss A, Durrant D, Chi NW, Lee RM. The cardiolipin-binding domain of Bid affects mitochondrial respiration and enhances cytochrome c release. Apoptosis 2004;9:533–41.
[53] Gonzalvez F, Pariselli F, Dupaigne P, Budihardjo I, Lutter M, Antonsson B, et al. tBid interaction with cardiolipin primarily orchestrates mitochondrial dysfunctions and subsequently activates Bax and Bak. Cell Death Differ 2005;12:614–26.
[54] Giordano A, Calvani M, Petillo O, Grippo P, Tuccillo F, Melone. et al. tBid induces alterations of mitochondrial fatty acid oxidation flux by malonyl-CoA-independent inhibition of carnitine palmitoyltransferase-1. Cell Death Differ 2005;12:603–13.
[55] Tyurin VA, Tyurina YY, Osipov AN, Belikova NA, Basova LV, Kapralov AA, et al. Interactions of cardiolipin and lyso-cardiolipins with cytochrome c and tBid: conflict or assistance in apoptosis. Cell Death Differ 2007;14:872–5.